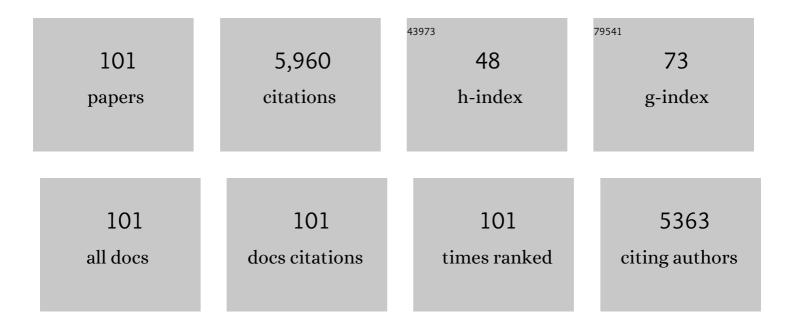
## Meiping Tong

List of Publications by Year in descending order

Source: https://exaly.com/author-pdf/9060078/publications.pdf Version: 2024-02-01



#	Article	IF	CITATIONS
1	Peroxymonosulfate enhanced photocatalytic degradation of serial bisphenols by metal-free covalent organic frameworks under visible light irradiation: mechanisms, degradation pathway and DFT calculation. Chemical Engineering Journal, 2022, 430, 132833.	6.6	15
2	Transport and deposition behaviors of microplastics in porous media: Co-impacts of N fertilizers and humic acid. Journal of Hazardous Materials, 2022, 426, 127787.	6.5	26
3	Improved removal performance of Gram-negative and Gram-positive bacteria in sand filtration system with arginine modified biochar amendment. Water Research, 2022, 211, 118006.	5.3	9
4	Insight into the role of Fe in the synergetic effect of persulfate/sulfite and Fe2O3@g-C3N4 for carbamazepine degradation. Science of the Total Environment, 2022, 819, 152787.	3.9	27
5	Catalyst-Free Periodate Activation by Solar Irradiation for Bacterial Disinfection: Performance and Mechanisms. Environmental Science & amp; Technology, 2022, 56, 4413-4424.	4.6	55
6	Photocatalytic degradation of paracetamol and bisphenol A by chitosan supported covalent organic framework thin film with visible light irradiation. Journal of Hazardous Materials, 2022, 435, 128966.	6.5	40
7	Bacterial capture and inactivation in sand filtration systems with addition of zero-valent iron as permeable layer under both slow and fast filtration conditions. Journal of Hazardous Materials, 2022, 436, 129122.	6.5	3
8	Freeze-thaw cycles induce diverse bacteria release behaviors from quartz sand columns with different water saturations. Water Research, 2022, 221, 118683.	5.3	5
9	Addition of biochar as thin preamble layer into sand filtration columns could improve the microplastics removal from water. Water Research, 2022, 221, 118783.	5.3	23
10	Activation of sulfite by single-atom Fe deposited graphitic carbon nitride for diclofenac removal: The synergetic effect of transition metal and photocatalysis. Chemical Engineering Journal, 2021, 407, 127167.	6.6	73
11	Different electrically charged proteins result in diverse transport behaviors of plastic particles with different surface charge in quartz sand. Science of the Total Environment, 2021, 756, 143837.	3.9	18
12	Facile synthesis of sulfhydryl modified covalent organic frameworks for high efficient Hg(II) removal from water. Journal of Hazardous Materials, 2021, 405, 124190.	6.5	46
13	Tunable Covalent Organic Frameworks with Different Heterocyclic Nitrogen Locations for Efficient Cr(VI) Reduction, <i>Escherichia coli</i> Disinfection, and Paracetamol Degradation under Visible-Light Irradiation. Environmental Science & Technology, 2021, 55, 5371-5381.	4.6	79
14	Flagella and Their Properties Affect the Transport and Deposition Behaviors of <i>Escherichia coli</i> in Quartz Sand. Environmental Science & Technology, 2021, 55, 4964-4973.	4.6	26
15	Ni <sub>1â^'</sub> <i><sub>x</sub></i> Co <i><sub>x</sub></i> Se <sub>2</sub> C/ZnIn <sub>2</sub> S <sub> Hybrid Nanocages with Strong 2D/2D Heteroâ€Interface Interaction Enable Efficient H<sub>2</sub>â€Releasing Photocatalysis. Advanced Functional Materials, 2021, 31, 2100923.</sub>	4 7.8	104
16	The degradation pathways of carbamazepine in advanced oxidation process: A mini review coupled with DFT calculation. Science of the Total Environment, 2021, 779, 146498.	3.9	88
17	Emerging Dualâ€Atomicâ€Site Catalysts for Efficient Energy Catalysis. Advanced Materials, 2021, 33, e2102576.	11.1	226
18	Different degradation mechanisms of carbamazepine and diclofenac by single-atom Barium embedded g-C3N4: the role of photosensitation-like mechanism. Journal of Hazardous Materials, 2021, 416, 125936.	6.5	43

#	Article	IF	CITATIONS
19	Transport and deposition of plastic particles in porous media during seawater intrusion and groundwater-seawater displacement processes. Science of the Total Environment, 2021, 781, 146752.	3.9	21
20	Bacteria have different effects on the transport behaviors of positively and negatively charged microplastics in porous media. Journal of Hazardous Materials, 2021, 415, 125550.	6.5	40
21	Insight into the synergetic effect of photocatalysis and transition metal on sulfite activation: Different mechanisms for carbamazepine and diclofenac degradation. Science of the Total Environment, 2021, 787, 147626.	3.9	21
22	Transport and deposition of microplastic particles in saturated porous media: Co-effects of clay particles and natural organic matter. Environmental Pollution, 2021, 287, 117585.	3.7	56
23	Transport behaviors of plastic particles in saturated quartz sand without and with biochar/Fe3O4-biochar amendment. Water Research, 2020, 169, 115284.	5.3	137
24	Cotransport and deposition of biochar with different sized-plastic particles in saturated porous media. Science of the Total Environment, 2020, 713, 136387.	3.9	52
25	Magnetic Fe3O4-deposited flower-like MoS2 nanocomposites for the Fenton-like Escherichia coli disinfection and diclofenac degradation. Journal of Hazardous Materials, 2020, 385, 121604.	6.5	116
26	Modification of zero valent iron nanoparticles by sodium alginate and bentonite: Enhanced transport, effective hexavalent chromium removal and reduced bacterial toxicity. Journal of Hazardous Materials, 2020, 388, 121822.	6.5	52
27	Different surface charged plastic particles have different cotransport behaviors with kaolinite âʿ†particles in porous media. Environmental Pollution, 2020, 267, 115534.	3.7	30
28	Agl modified covalent organic frameworks for effective bacterial disinfection and organic pollutant degradation under visible light irradiation. Journal of Hazardous Materials, 2020, 398, 122865.	6.5	73
29	Single-atom silver induced amorphization of hollow tubular g-C3N4 for enhanced visible light-driven photocatalytic degradation of naproxen. Science of the Total Environment, 2020, 742, 140642.	3.9	34
30	Influence of biofilm on the transport and deposition behaviors of nano- and micro-plastic particles in quartz sand. Water Research, 2020, 178, 115808.	5.3	65
31	Influence of titanium dioxide nanoparticles on the transport and deposition of microplastics in quartz sand. Environmental Pollution, 2019, 253, 351-357.	3.7	61
32	Cotransport of graphene oxides/reduced graphene oxides with BPA in both bare and iron oxides coated quartz sand. Science China Technological Sciences, 2019, 62, 1896-1906.	2.0	8
33	The influence of different charged poly (amido amine) dendrimer on the transport and deposition of bacteria in porous media. Water Research, 2019, 161, 364-371.	5.3	12
34	Cotransport and Deposition of Iron Oxides with Different-Sized Plastic Particles in Saturated Quartz Sand. Environmental Science & Technology, 2019, 53, 3547-3557.	4.6	95
35	Different mechanisms for E. coli disinfection and BPA degradation by CeO2-AgI under visible light irradiation. Chemical Engineering Journal, 2019, 371, 750-758.	6.6	64
36	Effects of graphene oxides on transport and deposition behaviors of bacteria in saturated porous media. Science China Technological Sciences, 2019, 62, 276-286.	2.0	6

#	Article	IF	CITATIONS
37	Photocatalytic removal of diclofenac by Ti doped BiOI microspheres under visible light irradiation: Kinetics, mechanism, and pathways. Journal of Molecular Liquids, 2019, 275, 807-814.	2.3	50
38	Bactericidal activity and mechanisms of BiOBr-AgBr under both dark and visible light irradiation conditions. Colloids and Surfaces B: Biointerfaces, 2018, 167, 275-283.	2.5	36
39	Sea-Buckthorn-Like MnO <sub>2</sub> Decorated Titanate Nanotubes with Oxidation Property and Photocatalytic Activity for Enhanced Degradation of 17β-Estradiol under Solar Light. ACS Applied Energy Materials, 2018, 1, 2123-2133.	2.5	34
40	Facile synthesis of magnetic Fe3O4@BiOI@AgI for water decontamination with visible light irradiation: Different mechanisms for different organic pollutants degradation and bacterial disinfection. Water Research, 2018, 137, 120-129.	5.3	117
41	Enhanced bacterial disinfection by Bi2MoO6-AgBr under visible light irradiation. Colloids and Surfaces B: Biointerfaces, 2018, 161, 528-536.	2.5	13
42	Efficient adsorption of Selenium(IV) from water by hematite modified magnetic nanoparticles. Chemosphere, 2018, 193, 134-141.	4.2	79
43	Influence of Nano- and Microplastic Particles on the Transport and Deposition Behaviors of Bacteria in Quartz Sand. Environmental Science & Technology, 2018, 52, 11555-11563.	4.6	32
44	Different electrically charged proteins result in diverse bacterial transport behaviors in porous media. Water Research, 2018, 143, 425-435.	5.3	33
45	Facile synthesis of ZrO2 coated BiOCl0.510.5 for photocatalytic oxidation-adsorption of As(III) under visible light irradiation. Chemosphere, 2018, 211, 934-942.	4.2	16
46	Enhanced visible-light-driven photocatalytic bacteria disinfection by g-C 3 N 4 -AgBr. Colloids and Surfaces B: Biointerfaces, 2017, 152, 49-57.	2.5	94
47	Stability of carboxyl-functionalized carbon black nanoparticles: the role of solution chemistry and humic acid. Environmental Science: Nano, 2017, 4, 800-810.	2.2	42
48	Influence of Bisphenol A on the transport and deposition behaviors of bacteria in quartz sand. Water Research, 2017, 121, 1-10.	5.3	32
49	Influence of graphene oxide on the transport and deposition behaviors of colloids in saturated porous media. Environmental Pollution, 2017, 225, 141-149.	3.7	56
50	Efficient bacterial inactivation with Z-scheme AgI/Bi2MoO6 under visible light irradiation. Water Research, 2017, 123, 632-641.	5.3	116
51	Effect of bacteria on the transport and deposition of multi-walled carbon nanotubes in saturated porous media. Environmental Pollution, 2016, 213, 895-903.	3.7	25
52	Bactericidal activity and mechanism of Ti-doped BiOI microspheres under visible light irradiation. Colloids and Surfaces B: Biointerfaces, 2016, 147, 307-314.	2.5	36
53	Effect of different-sized colloids on the transport and deposition of titanium dioxide nanoparticles in quartz sand. Environmental Pollution, 2016, 208, 637-644.	3.7	43
54	Influence of Perfluorooctanoic Acid on the Transport and Deposition Behaviors of Bacteria in Quartz Sand. Environmental Science & Technology, 2016, 50, 2381-2388.	4.6	37

#	Article	IF	CITATIONS
55	Bactericidal activity and mechanism of AgI/AgBr/BiOBr0.7510.25 under visible light irradiation. Colloids and Surfaces B: Biointerfaces, 2016, 138, 102-109.	2.5	34
56	Cotransport of bacteria with hematite in porous media: Effects of ion valence and humic acid. Water Research, 2016, 88, 586-594.	5.3	50
57	Bactericidal mechanisms of Au@TNBs under visible light irradiation. Colloids and Surfaces B: Biointerfaces, 2015, 128, 211-218.	2.5	19
58	Bactericidal mechanism of BiOl–AgI under visible light irradiation. Chemical Engineering Journal, 2015, 279, 277-285.	6.6	81
59	Efficient removal of free and nitrilotriacetic acid complexed Cd(II) from water by poly(1-vinylimidazole)-grafted Fe3O4@SiO2 magnetic nanoparticles. Journal of Hazardous Materials, 2015, 299, 479-485.	6.5	18
60	Influence of gravity on transport and retention of representative engineered nanoparticles in quartz sand. Journal of Contaminant Hydrology, 2015, 181, 153-160.	1.6	28
61	Fe <sub>5</sub> C <sub>2</sub> nanoparticles: a reusable bactericidal material with photothermal effects under near-infrared irradiation. Journal of Materials Chemistry B, 2015, 3, 3993-4000.	2.9	37
62	Efficient bacteria capture and inactivation by cetyltrimethylammonium bromide modified magnetic nanoparticles. Colloids and Surfaces B: Biointerfaces, 2015, 136, 659-665.	2.5	47
63	Removal of Hg(II) by poly(1-vinylimidazole)-grafted Fe3O4@SiO2 magnetic nanoparticles. Water Research, 2015, 69, 252-260.	5.3	175
64	Toxicity of TiO2 Nanoparticles to Escherichia coli: Effects of Particle Size, Crystal Phase and Water Chemistry. PLoS ONE, 2014, 9, e110247.	1.1	156
65	Influence of silicate on the transport of bacteria in quartz sand and iron mineral-coated sand. Colloids and Surfaces B: Biointerfaces, 2014, 123, 995-1002.	2.5	24
66	Influence of sulfate and phosphate on the deposition of plasmid DNA on silica and alumina-coated surfaces. Colloids and Surfaces B: Biointerfaces, 2014, 118, 83-89.	2.5	6
67	Aggregation and dissolution of ZnO nanoparticles synthesized by different methods: Influence of ionic strength and humic acid. Colloids and Surfaces A: Physicochemical and Engineering Aspects, 2014, 451, 7-15.	2.3	85
68	Efficient removal of trace antimony(III) through adsorption by hematite modified magnetic nanoparticles. Journal of Hazardous Materials, 2014, 268, 229-236.	6.5	148
69	Efficient bacterial capture with amino acid modified magnetic nanoparticles. Water Research, 2014, 50, 124-134.	5.3	125
70	Influence of Clay Particles on the Transport and Retention of Titanium Dioxide Nanoparticles in Quartz Sand. Environmental Science & Technology, 2014, 48, 7323-7332.	4.6	112
71	Cotransport of multi-walled carbon nanotubes and titanium dioxide nanoparticles in saturated porous media. Environmental Pollution, 2014, 195, 31-38.	3.7	42
72	Transport and retention behaviors of titanium dioxide nanoparticles in iron oxide-coated quartz sand: Effects of pH, ionic strength, and humic acid. Colloids and Surfaces A: Physicochemical and Engineering Aspects, 2014, 454, 119-127.	2.3	76

#	Article	IF	CITATIONS
73	Enhanced removal of trace arsenate by magnetic nanoparticles modified with arginine and lysine. Chemical Engineering Journal, 2014, 254, 340-348.	6.6	35
74	Facile self-assembly synthesis of titanate/Fe <sub>3</sub> O <sub>4</sub> nanocomposites for the efficient removal of Pb <sup>2+</sup> from aqueous systems. Journal of Materials Chemistry A, 2013, 1, 805-813.	5.2	89
75	Initial transport and retention behaviors of ZnO nanoparticles in quartz sand porous media coated with Escherichia coli biofilm. Environmental Pollution, 2013, 174, 38-49.	3.7	63
76	Effect of Carbon Nanotubes on the Transport and Retention of Bacteria in Saturated Porous Media. Environmental Science & Technology, 2013, 47, 11537-11544.	4.6	32
77	Efficient removal of trace arsenite through oxidation and adsorption by magnetic nanoparticles modified with Fe–Mn binary oxide. Water Research, 2013, 47, 3411-3421.	5.3	196
78	Bactericidal mechanisms of Ag2O/TNBs under both dark and light conditions. Water Research, 2013, 47, 1837-1847.	5.3	67
79	Influence of sulfate on the transport of bacteria in quartz sand. Colloids and Surfaces B: Biointerfaces, 2013, 110, 443-449.	2.5	13
80	Bactericidal activity of Ag-doped multi-walled carbon nanotubes and the effects of extracellular polymeric substances and natural organic matter. Colloids and Surfaces B: Biointerfaces, 2013, 104, 133-139.	2.5	36
81	Cotransport of Titanium Dioxide and Fullerene Nanoparticles in Saturated Porous Media. Environmental Science & Technology, 2013, 47, 5703-5710.	4.6	78
82	Influence of nutrient conditions on the transport of bacteria in saturated porous media. Colloids and Surfaces B: Biointerfaces, 2013, 102, 752-758.	2.5	36
83	Influence of Bentonite Particles on Representative Gram Negative and Gram Positive Bacterial Deposition in Porous Media. Environmental Science & Technology, 2012, 46, 11627-11634.	4.6	51
84	Removal of arsenate by cetyltrimethylammonium bromide modified magnetic nanoparticles. Journal of Hazardous Materials, 2012, 227-228, 461-468.	6.5	115
85	Transport and deposition of ZnO nanoparticles in saturated porous media. Colloids and Surfaces A: Physicochemical and Engineering Aspects, 2012, 401, 29-37.	2.3	109
86	Influence of humic acid on the transport behavior of bacteria in quartz sand. Colloids and Surfaces B: Biointerfaces, 2012, 91, 122-129.	2.5	78
87	Deposition kinetics of MS2 bacteriophages on clay mineral surfaces. Colloids and Surfaces B: Biointerfaces, 2012, 92, 340-347.	2.5	32
88	Influence of natural organic matter on the deposition kinetics of extracellular polymeric substances (EPS) on silica. Colloids and Surfaces B: Biointerfaces, 2011, 87, 151-158.	2.5	29
89	Influence of solution chemistry on the deposition and detachment kinetics of RNA on silica surfaces. Colloids and Surfaces B: Biointerfaces, 2011, 82, 443-449.	2.5	13
90	Deposition kinetics of zinc oxide nanoparticles on natural organic matter coated silica surfaces. Journal of Colloid and Interface Science, 2010, 350, 427-434.	5.0	67

#	Article	IF	CITATIONS
91	Contribution of Extracellular Polymeric Substances on Representative Gram Negative and Gram Positive Bacterial Deposition in Porous Media. Environmental Science & Technology, 2010, 44, 2393-2399.	4.6	55
92	Influence of biofilm on the transport of fullerene (C60) nanoparticles in porous media. Water Research, 2010, 44, 1094-1103.	5.3	77
93	Deposition Kinetics of Extracellular Polymeric Substances (EPS) on Silica in Monovalent and Divalent Salts. Environmental Science & Technology, 2009, 43, 5699-5704.	4.6	68
94	Influence of Extracellular Polymeric Substances (EPS) on Deposition Kinetics of Bacteria. Environmental Science & Technology, 2009, 43, 2308-2314.	4.6	122
95	Comment on "Transport and fate of bacteria in porous media: Coupled effects of chemical conditions and pore space geometry―by Saeed Torkzaban et al Water Resources Research, 2009, 45, .	1.7	17
96	Funneling of Flow into Grain-to-grain Contacts Drives Colloidâ^'Colloid Aggregation in the Presence of an Energy Barrier. Environmental Science & Technology, 2008, 42, 2826-2832.	4.6	79
97	Colloid Population Heterogeneity Drives Hyperexponential Deviation from Classic Filtration Theory. Environmental Science & Technology, 2007, 41, 493-499.	4.6	98
98	On colloid retention in saturated porous media in the presence of energy barriers: The failure of <i>α</i> , and opportunities to predict <i>η</i> . Water Resources Research, 2007, 43, .	1.7	36
99	Excess Colloid Retention in Porous Media as a Function of Colloid Size, Fluid Velocity, and Grain Angularity. Environmental Science & Technology, 2006, 40, 7725-7731.	4.6	136
100	Spatial Variation in Deposition Rate Coefficients of an Adhesion-Deficient Bacterial Strain in Quartz Sand. Environmental Science & Technology, 2005, 39, 3679-3687.	4.6	55
101	Detachment-Influenced Transport of an Adhesion-Deficient Bacterial Strain within Water-Reactive Porous Media, Environmental Science & amp: Technology, 2005, 39, 2500-2508.	4.6	75